Structural Eng. / Earthquake Eng. Vol. 3. No. 2, 267s-275s. October 1986
Japan Society of Civil Engineers (Proc. of JSCE No. 374/I-6)

INVERSE SCATTERING OF ELASTIC WAVES FOR A CAVITY

By Yoshiji NIWA and Sohichi HIROSE***

The inverse scattering problems of determining the shape of a cavity from observed waves are investigated by means of the Born inversion. The far-field amplitude of scattered waves is related to the spatial Fourier transform of a characteristic function of a cavity, which is equal to unity in the region occupied by a cavity and zero elsewhere. However, this method is based on the long-wavelength approximation, and is not adequate to the high frequency data. To improve the accuracy of inversion, we further propose the modified Born inversion which is applicable even for the high frequency data. In numerical examples, the data synthesized by the boundary integral equation are used to check the effect of some factors of incident and observed waves on the imaging of a cavity.

Keywords: *inverse scattering, born approximation, elastic wave*

1. INTRODUCTION

Problems of wave scattering are mainly classified into two groups. The one is the forward scattering problems, which are concerned with the determination of the response when the shape and medium property of a scatterer are given. The other is the inverse scattering problems, which deal with the finding of the shape and medium property of a scatterer from the response observed at a few locations.

As reviewed by Pao[1], the major progress on the analysis of forward scattering problems has been made. Among several numerical methods, particularly, the integral equation method, which seems to be the most effective in elastodynamics, has been well developed and applied to various forward problems of elastic waves[2)~4)].

Inverse problems are originally measurement problems which may occur in various research fields such as seismology, ocean acoustics, ultrasonic nondestructive testing, biomedical ultrasonics, and so forth. Therefore the algorithms of inversion depend crucially on recording techniques of scattering data and the structure of the incident field. For this reason, even though many algorithms on inverse problems have been proposed as the case may be, there seems to be no unified method for all of them[5)].

Among a variety of inversion algorithms, the POFFIS (Physical Optics Far-Field Inverse Scattering) and Born inversion are a couple of widely used methods. The former is for high frequency data, and the latter is based on the low frequency assumption. In acoustics, the POFFIS has been elaborately investigated by several authors[6)~9)]. Furthermore, Achenbach et al.[10)] applied an analogous approximation (Physical Elastodynamics Far-Field Inverse Scattering) to crack-scattering data of elastic waves. On the other hand, the Born inversion has been studied both experimentally and theoretically by Rose and

* Member of JSCE, Dr. Eng., President, Fukui Technical College. (Sabae, Fukui 916)
** Member of JSCE, M. Eng., Instructor, Department of Civil Engineering, Kyoto University. (Sakyo-ku, Kyoto 606)

Krumhansl[11] and Hsu et al[12]. They used the one dimensional Born inversion algorithm to characterize an inclusion in elastic media.

In this paper, we investigate the Born inversion for scattering of elastic waves by a cavity, and modify the approach to improve the accuracy of Born approximation in the high frequency range. In numerical examples, the scattered data calculated by the boundary integral equation are used to examine the effect of several factors of incident and observed waves on the reconstructed shape of a cavity.

2. INVERSE SCATTERING PROBLEM FOR A CAVITY

Let us consider an infinite body D with a cavity V in a two dimensional space, as shown in Fig. 1. For convenience, the origin o is placed in the region V. Under the assumptions of infinitesimal deformation and linear elastic, isotropic and homogeneous material behavior, the equations of motion for the body D are

$$C_{ijmn}u_{m,nj}(\boldsymbol{x})+\rho\omega^2 u_i(\boldsymbol{x})+b_i(\boldsymbol{x})=0 \qquad \boldsymbol{x} \text{ in D} \quad \cdots\cdots (1)$$

where u_i, b_i, C_{ijmn}, ρ and ω are displacement, body force, elastic moduli, mass density and angular frequency, respectively. From the assumption of isotropy and homogeneity of material, C_{ijmn} are expressed by Lamé constants λ and μ as follows

$$C_{ijmn}=\lambda\delta_{ij}\delta_{mn}+\mu(\delta_{im}\delta_{jn}+\delta_{in}\delta_{jm}). \quad \cdots\cdots (2)$$

The boundary condition on the surface S of a cavity V is written as

$$t_i(\boldsymbol{x})\equiv n_j C_{ijmn}u_{m,n}(\boldsymbol{x})=0 \qquad \boldsymbol{x} \text{ on S} \quad \cdots\cdots (3)$$

where n_j is a unit vector normal to the boundary S. Furthermore, the scattered field u_i^{sc}, which is defined as $u_i^{sc}\equiv u_i-u_i^{in}$ (u_i^{in} : incident field), satisfies the Sommerfeld radiation condition at infinity.

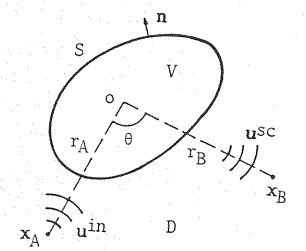

Fig. 1 A cavity in an infinite body.

The forward scattering problem is stated as

to determine a solution of eq. (1), subjected to the boundary condition (3) and the radiation condition at infinity, when the incident wave field and the shape of a cavity V are given.

This problem is a well-posed problem, for which a wealth of knowledge has been accumulated. In contrast, not much is known about the solutions for inverse problems of elastic waves, and there exists no unified analysis for them. In such a sense, the present paper deals with the special class of inverse problems, i.e., the finding of a shape of a cavity V when the incident wave field is known and some data of the scattered fields are given. To solve this problem, however, we need additional constraints on the incident wave field and the observed waves as follows

(1) The incident wave is assumed to be a cylindrical wave emitted from the source point $\boldsymbol{x}_A$. That is to say, the body force $b_i(\boldsymbol{x})$ is a point force given as

$$b_i(\boldsymbol{x})=f_i\delta(\boldsymbol{x}-\boldsymbol{x}_A)$$

where f_i denotes the direction of a point force and $\delta(\boldsymbol{x})$ is the Dirac delta function. Then the incident wave $u_i^{in}(\boldsymbol{x}, \boldsymbol{x}_A)$ can be expressed by

$$u_i^{in}(\boldsymbol{x}, \boldsymbol{x}_A)=U_i^k(\boldsymbol{x}, \boldsymbol{x}_A)f_k$$

where U_i^k is the fundamental solution defined later (see eq. (5)).

(2) The scattered wave is observed at the other point $\boldsymbol{x}_B$ and in band-limited frequencies.

(3) In the simulation analysis, a series of pitch-catch tests around a cavity are carried out on condition that the distances, r_A and r_B, from the source and observation points to a cavity are large compared to the size of a cavity, and the angle θ between the vectors $\boldsymbol{x}_A$ and $\boldsymbol{x}_B$ holds constant.

3. FORMULATION OF INTEGRAL EQUATION

To facilitate the analysis of inverse scattering problems, we briefly review the formulation of the intergral equation in elastodynamics.

(1) Fundamental solution

We begin with the fundamental solution which satisfies the following equation

$$C_{ijmn}U^k_{m,nj}(\boldsymbol{x},\boldsymbol{y})+\rho\omega^2 U^k_i(\boldsymbol{x},\boldsymbol{y})=-\delta_{ik}\delta(\boldsymbol{x}-\boldsymbol{y}) \quad (4)$$

where δ_{ik} is the Kronecker delta. $U^k_i(\boldsymbol{x},\boldsymbol{y})$ indicates the displacement in the i-direction at $\boldsymbol{x}$ due to a point unit force in the k-direction at $\boldsymbol{y}$. For an isotropic, homogeneous elastic medium in a two dimensional space, $U^k_i(\boldsymbol{x},\boldsymbol{y})$ is well-known in the explicit form

$$U^k_i(\boldsymbol{x},\boldsymbol{y})=\frac{i}{4\mu}[H^{(1)}_0(k_T r)\,\delta_{ik}+k_T^{-2}\partial_i\partial_k\{H^{(1)}_0(k_T r)-H^{(1)}_0(k_L r)\}] \quad (5)$$

where $H^{(1)}_0(\cdot)$ is the zero-order Hankel function of the first kind and $r=|\boldsymbol{x}-\boldsymbol{y}|$. k_T and k_L are the transverse and longitudinal wave numbers, respectively.

(2) Integral representation for the displacement

By applying the exterior Green's formula to the scattered field in the region D and the interior Green's formula to the incident field in the region V, the scattered wave u^{sc}_i at the point $\boldsymbol{x}_B$ in D is expressed by the following integral equation,

$$u^{sc}_i(\boldsymbol{x}_B)=\int_S n_j(\boldsymbol{y})\,C_{kjmn}U^{m,n}_i(\boldsymbol{x}_B,\boldsymbol{y})\,u_k(\boldsymbol{y})\,dS_y \qquad \boldsymbol{x}_B \text{ in D} \quad (6)$$

where the superscript $,n$ indicates the differential with respect to the second argument of U^m_i, i.e., $\partial U^m_i(\boldsymbol{x}_B,\boldsymbol{y})/\partial y_n$. In the derivation of eq. (6), the boundary condition (3) is taken into account.

From the limiting procedure, $\boldsymbol{x}_B$ in D to the boundary point $\boldsymbol{x}_0$ on S, furthermore, we have the boundary integral equation[2)~4)]

$$(\delta_{ij}-c^e_{ij})\,u_j(\boldsymbol{x}_0)=u^{in}_i(\boldsymbol{x}_0,\boldsymbol{x}_A)+\int\!\!\!\!\!\!-_S n_j(\boldsymbol{y})\,C_{kjmn}U^{m,n}_i(\boldsymbol{x}_0,\boldsymbol{y})\,u_k(\boldsymbol{y})\,dS_y \qquad \boldsymbol{x}_0 \text{ on S} \quad (8)$$

where $c^e_{ij}u_j$ denotes the free term of the exterior limit of the double layer potential and a slash through the integration symbol indicates the principal value integral. We can use eq. (8) in order to solve forward scattering problems.

4. INVERSE SCATTERING BASED ON THE BORN APPROXIMATION

(1) Characteristic function and its Fourier transform

We now introduce the characteristic function of the domain V, defined as[9)]

$$\gamma(\boldsymbol{x})=\begin{cases}1 & \boldsymbol{x} \text{ in V}\\ 0 & \boldsymbol{x} \text{ in D}\end{cases} \quad (9)$$

The spatial Fourier transform of $\gamma(\boldsymbol{x})$ is defined by

$$\Gamma(\boldsymbol{\xi})=\int_{V+D}\gamma(\boldsymbol{x})\exp(-i\boldsymbol{\xi}\cdot\boldsymbol{x})\,dS_x$$
$$=\int_V \exp(-i\boldsymbol{\xi}\cdot\boldsymbol{x})\,dS_x \quad (10)$$

If we obtain $\Gamma(\boldsymbol{\xi})$ from observations of scattered waves, the inverse Fourier transform

$$\gamma(\boldsymbol{x})=\frac{1}{(2\pi)^2}\int\Gamma(\boldsymbol{\xi})\exp(i\boldsymbol{\xi}\cdot\boldsymbol{x})\,d\boldsymbol{\xi} \quad (11)$$

yields the characteristic function which represents a shape of a cavity V to be determined.

(2) Born inversion

The Born approximation, which is often used in scattering theory[13)], replaces the exact displacement on the boundary S by the incident fields. Then eq. (6) becomes

$$u^{sc}_i(\boldsymbol{x}_B)=\int_S n_j(\boldsymbol{y})\,C_{kjmn}U^{m,n}_i(\boldsymbol{x}_B,\boldsymbol{y})\,u^{in}_k(\boldsymbol{y},\boldsymbol{x}_A)\,dS_y. \quad (12)$$

Furthermore, applying the divergence theorem to eq. (12) yields

$$u^{sc}_i(\boldsymbol{x}_B)=\int_V\{C_{kjmn}U^{m,n}_i(\boldsymbol{x}_B,\boldsymbol{y})\,u^{in}_{k,j}(\boldsymbol{y},\boldsymbol{x}_A)-\rho\omega^2 U^k_i(\boldsymbol{x}_B,\boldsymbol{y})\,u^{in}_k(\boldsymbol{y},\boldsymbol{x}_A)\}\,dS_y. \quad (13)$$

From the assumption, the point $\boldsymbol{x}_B$ is far from the cavity. Therefore, if only the leading order terms of Hankel function in the fundamental solution are retained in eq. (13), we have

$$u_i^{sc}(\boldsymbol{x}_B)=-i\Lambda(k_L, r_B)\hat{x}_{Bi}\hat{x}_{Bj}\Phi_j(k_L)-i\Lambda(k_T, r_B)(\delta_{ij}-\hat{x}_{Bi}\hat{x}_{Bj})\Phi_j(k_T) \quad (14)$$

where $\hat{\boldsymbol{x}}_B$ denotes the unit vector $\boldsymbol{x}_B/|\boldsymbol{x}_B|$ and $\Phi_j(k)$ and $\Lambda(k, r)$ are defined as

$$\Phi_j(k)=\frac{k^2}{4\rho\omega^2}\left\{\rho\omega^2\int_V u_j^{in}(\boldsymbol{y}, \boldsymbol{x}_A)\exp(-ik\hat{\boldsymbol{x}}_B\cdot\boldsymbol{y})\,dS_y+ik\hat{x}_{Bk}C_{jkmn}\int_V \varepsilon_{mn}^{in}(\boldsymbol{y}, \boldsymbol{x}_A)\exp(-ik\hat{\boldsymbol{x}}_B\cdot\boldsymbol{y})\,dS_y\right\}$$

$$\Lambda(k, r)=\sqrt{2}/(\pi kr)^{1/2}\exp(ikr-i\pi/4)$$

$$\varepsilon_{mn}^{in}(\boldsymbol{y}, \boldsymbol{x}_A)=\frac{1}{2}\{u_{m,n}^{in}(\boldsymbol{y}, \boldsymbol{x}_A)+u_{n,m}^{in}(\boldsymbol{y}, \boldsymbol{x}_A)\}.$$

The right-hand side of eq. (14) is of the form of two outgoing cylindrical waves, one with a P wave speed and polarized longitudinally and the other with an SV wave speed and polarized transversely.

Now we consider the scattered field of longitudinal motion due to the longitudinal point force (P to P scattering), in which case the direction of a source force f_i is given by $f_i=\hat{x}_{Ai}$. Noticing that the distance r_A from the source to a cavity is large compared to the size of a cavity, the scattered P wave at the point $\boldsymbol{x}_B$ is expressed as

$$\begin{aligned}u_P^{sc}(\boldsymbol{x}_B)&=k_L^4/(4\rho\omega^2)^2\Lambda(k_L, r_A)\Lambda(k_L, r_B)(\rho\omega^2\hat{x}_{Aj}\hat{x}_{Bj}\\&\quad+k_L^2C_{jkmn}\hat{x}_{Am}\hat{x}_{An}\hat{x}_{Bj}\hat{x}_{Bk})\int_V\exp(-ik_L(\hat{\boldsymbol{x}}_A+\hat{\boldsymbol{x}}_B)\cdot\boldsymbol{y})\,dS_y\\&\equiv\Psi_{P\rho}\int_V\exp(-ik_L\boldsymbol{\zeta}\cdot\boldsymbol{y})\,dS_y \quad (15)\end{aligned}$$

where $\boldsymbol{\zeta}=\hat{\boldsymbol{x}}_A+\hat{\boldsymbol{x}}_B$. A comparison of eqs. (10) and (15) reveals that the two integrals differ only in the exponential factor. Therefore we can rewrite the characteristic function as an integral in cylindrical coordinates with the wave number k_L and the argument α of the vector ζ. The result is

$$\begin{aligned}\gamma(\boldsymbol{x})&=\frac{1}{(2\pi)^2}\int u_\rho^{sc}(\boldsymbol{x}_B)\Psi_{\rho\rho}^{-1}\exp(ik_L\boldsymbol{\zeta}\cdot\boldsymbol{x})\,d(k_L\boldsymbol{\zeta})\\&=\frac{1}{(2\pi)^2}\int_0^\infty\int_0^{2\pi}u_\rho^{sc}(\boldsymbol{x}_B)\Psi_{\rho\rho}^{-1}\exp(ik_L\boldsymbol{\zeta}(\alpha)\cdot\boldsymbol{x})\,k_L|\boldsymbol{\zeta}|^2\,d\alpha dk_L. \quad (16)\end{aligned}$$

Similarly to the case of the scattering of P to P wave as above-mentioned, we can also formulate the Born inversion for the other cases, such as SV to SV wave, SH to SH wave, and so on.

(3) Modified Born inversion

Originally, the Born approximation is valid for wave field in the low frequency range. Therefore, the Born inversion becomes no longer valid for the data of high frequency. To overcome this difficulty, we show a slight modification of the Born inversion in the following. Keeping in mind that the total displacement on the boundary S is expressed by

$$u_i(\boldsymbol{x})=u_i^{sc}(\boldsymbol{x})+u_i^{in}(\boldsymbol{x}) \qquad \boldsymbol{x} \text{ on S},$$

eq. (6) becomes

$$u_i^{sc}(\boldsymbol{x}_B)-\int_S n_j(\boldsymbol{y})C_{kjmn}U_i^{m,n}(\boldsymbol{x}_B, \boldsymbol{y})u_k^{sc}(\boldsymbol{y})\,dS_y=\int_S n_j(\boldsymbol{y})C_{kjmn}U_i^{m,n}(\boldsymbol{x}_B, \boldsymbol{y})u_k^{in}(\boldsymbol{y})\,dS_y. \quad (17)$$

In Born inversion, we neglect the integral on the left-hand side in eq. (17), assuming that the effect of scattered waves is small. The procedure of the modified Born inversion is as follows.

- First of all, solve the Born inversion and locate the boundary as the first approximate value.
- Using the boundary determined above, analyze the forward scattering problem by means of eq. (8) and calculate the scattered waves on the boundary S.
- Evaluate the left-hand side of eq. (17).
- Again solve the inverse problem with the left-hand side of eq. (17) as a known quantity.

(4) One dimensional problem

If the cavity V is beforehand known as a circular cylindrical region, the problem is reduced to one dimensional problem which is concerned with determining the radius of a circular cavity. In this case, the factor $u_\rho^{sc}(\boldsymbol{x}_B)\Psi_{\rho\rho}^{-1}$ in eq. (16) is free from the parameter α. Therefore, eq. (16) is rewritten as

$$\gamma(|x|)=\frac{1}{(2\pi)^2}\int_0^{\infty} u_P^{sc}(x_B)\,\mathcal{F}_{PP}^{-1}k_L|\zeta|^2\int_0^{2\pi}\exp(ik_L\zeta(\alpha)\cdot x)\,d\alpha dk_L$$

$$=\frac{1}{2\pi}\int_0^{\infty} k_L|\zeta|^2 u_P^{sc}(x_B)\,\mathcal{F}_{PP}^{-1}J_0(k_L|\zeta||x|)\,dk_L \quad \cdots\cdots (18)$$

where $J_0(\cdot)$ is the zero-order Bessel function.

5. APPLICATION OF THE INVERSION TECHNIQUE TO NUMERICAL EXAMPLES

We now show the application of the inversion technique to numerical examples. The scattered waves observed at the point x_B are calculated by the preliminary numerical analysis using the boundary integral equation (8). In the following examples, the Poisson's ratio of the body D is assumed to be 0.25.

First we take one dimensional problems in order to examine the effect of several factors on the accuracy of inversion technique. Next we show some examples for cavities in a two dimensional space.

(1) One dimensional problems

a) Effect of band limiting of frequency

In numerical analysis, the improper integral of eq. (18) is truncated in a band limit from $(k_L)_{\min}$ to $(k_L)_{\max}$. Figs. 2 and 3 show the radial distribution of characteristic functions for various band-limited data. In these figures, dashed lines represent the ideal characteristic function to be determined. All these examples are carried out on the following conditions,

- $r_A=r_B=5\,a$ (a : radius of a cavity).
- The pulse-echo scattering of P to P wave is carried out.
- The Born inversion is used.

In Fig. 2, we can see only a slight difference among the reconstructed results. Therefore the data in the high frequency range have a small effect on the distribution of characteristic function. In contrast, Fig. 3 shows that the lack of the low frequency data causes the great inaccuracy of the obtained results. This is because the characteristic function depends critically on the Fourier spectra in the low frequency.

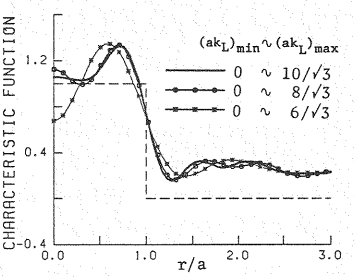

Fig. 2 Characteristic functions calculated for several band-limited data. (pulse-echo scattering of P to P wave, Born inversion, $r_A=r_B=5\,a$)

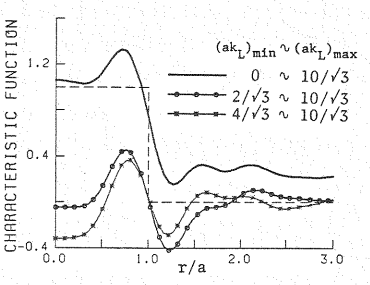

Fig. 3 The same as in Fig. 2.

b) Effect of the angle between source and observation points

We next test the effect of the angle θ between source and observation points. Fig. 4 presents the characteristic functions for the P to P scattering with several angles. Other parameters used are as follows,

- $r_A=r_B=5\,a$.
- The Born inversion is used.
- The frequency range considered is $0\leqq ak_T\leqq 10$.

Fig. 4 shows that the result for the pulse-echo

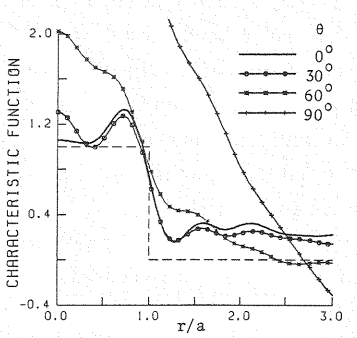

Fig. 4 Characteristic functions calculated for the pitch-catch scattering with various angles. (P to P wave scattering, Born inversion, $r_A=r_B=5\,a$, bandwidth of $0\leqq ak_T\leqq 10$)

data ($\theta=0^\circ$) agrees best with the ideal dashed line. Whereas the characteristic function is no longer reproduced when the angle θ is beyond 90°. There are two reasons for these phenomena. One is that the effective integral interval in eq. (18) becomes narrow for $\theta>90^\circ$ since the value $|\zeta|$ is small for a large angle. The other is that the amplitudes of scattered waves decrease rapidly for the angle θ beyond 90° as shown in Fig. 5. Fig. 5 depicts the radiation pattern of scattered P wave in the low frequency subjected to the incident P wave. These two reasons make the accuracy of inversion for $\theta>90^\circ$ degenerate.

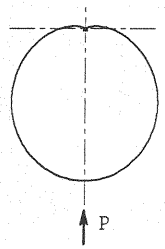

Fig. 5 Polar diagram of a radiation pattern of a scattered P wave in a low frequency subjected to an incident P wave.

c) Effect of distances from source and observation points to a cavity

To examine the validity of the far-field approximation, we show some examples for a variety of distances r_A and r_B as shown in Fig. 6. In these numerical simulations, we make the following remarks,

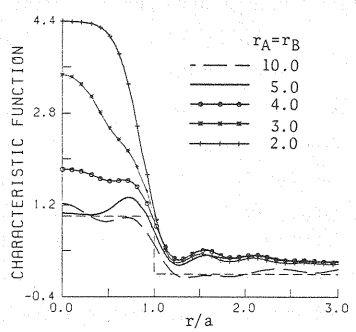

Fig. 6 Characteristic functions calculated for a variety of distances between source/observation points and a cavity. (Born inversion, bandwidth of $0\leqq ak_T\leqq 10$, pulse-echo scattering of P to P wave)

- $r_A=r_B$.
- The Born inversion is employed.
- The frequency bandwidth from $(ak_T)_{\min}=0$ to $(ak_T)_{\max}=10$ is used.
- The pulse-echo scattering of P to P wave is conducted.

Fig. 6 shows that the far-field approximation holds true when $r_A=r_B>5\,a$. On the other hand, an agreement between the synthesized characteristic function and the original one becomes worse in the region $r/a<1$, as source and observation points are nearer to a cavity. Apart from the quantities of the obtained results, however, the boundary of a cavity is detectable even if the near-field data are used.

d) Effect of mode conversion

Since SH wave is independent of P and SV waves in two dimensional motions, five types of mode conversion may occur, i.e., P-P, P-SV, SV-P, SV-SV and SH-SH. In Figs. 7 (a) to (c), we consider the cases of P-P, SV-SV, SH-SH mode conversions, respectively. The parameters used in these calculations are as follows,

- $r_A=r_B=5\,a$.
- The Born inversion is used.
- The frequency bandwidth is $0\leqq ak_T\leqq 10$.
- The pulse-echo scattering is carried out.

As shown in Fig. 7, the accuracy of Born inversion for inplane motions (P and SV waves) is worse than the accuracy for antiplane motion (SH wave). This is due to the fact that no mode conversion occurs in the case of antiplane motion, while there are mode conversions between P and SV waves. We here consider the P-P scattering as an example. Actually, the incident wave from the point force at $\boldsymbol{x}_A$ includes an SV wave as well as a P wave. Furthermore, the scattered wave observed at the point $\boldsymbol{x}_B$ has not only the component of a P wave but also the one of an SV wave. However, in the analysis of Born inversion, all of these SV waves are neglected due to the far-field approximation (see eq. (15)).

e) Born inversion vs. modified Born inversion

We here show the comparison between the Born inversion and the modified Born inversion. The results are shown in Figs. 8 (a) to (c) corresponding to the cases of P to P, SV to SV and SH to SH scattering,

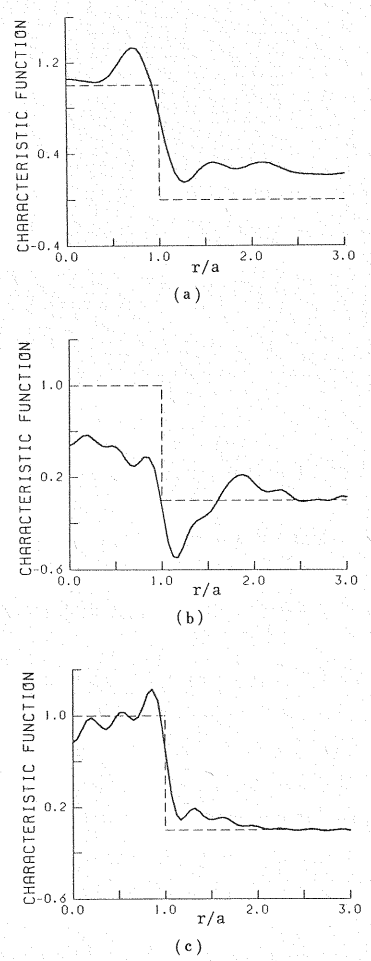

Fig. 7 Calculated characteristic functions for the cases of (a) P to P, (b) SV to SV, (c) SH to SH wave scattering. ($r_A = r_B = 5\,a$, Born inversion, bandwidth of $0 \leqq ak_T \leqq 10$, pulse-echo scattering)

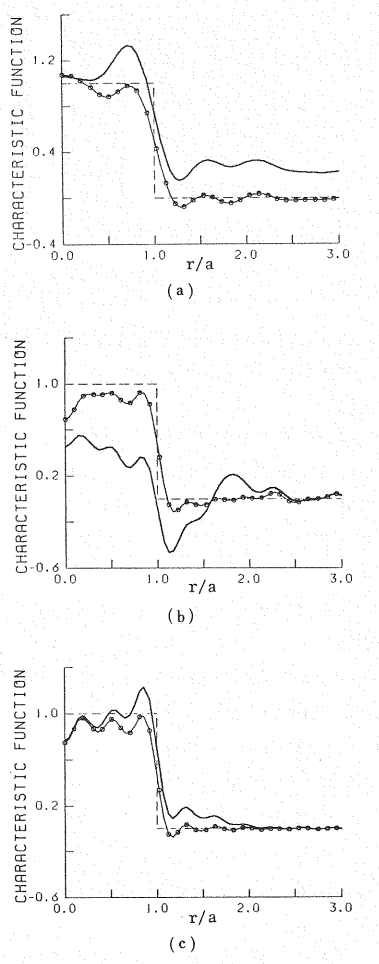

Fig. 8 Characteristic functions calculated by Born inversion (——) and modified Born inversion (⟜—⟜) ; (a) P to P, (b) SV to SV, (c) SH to SH wave scattering. Other parameters used are the same as in Fig. 7.

respectively. The parameters used are the same as in Fig. 7. From these figures, it is shown that the modified method improves the results with respect to oscillating lobes, which are related to high frequency data. Moreover, the modified Born inversion eliminates the errors caused by mode conversions of inplane motions as shown in Figs. 7 (a) and (b).

f) Summary of one dimensional analysis

From numerical analysis of one dimensional problems, it is mainly concluded that

- In the Born inversion, the low frequency data play an important role in reconstructing the characteristic function. On the other hand, the high frequency data have little effect on the imaging of a cavity.
- The pulse-echo method, where the observation point coincides with the source point, is more accurate than the pitch-catch method with θ not equal to zero.
- The Born inversion for inplane motions is less valid than the inversion for antiplane motions, because there are mode conversions between P and SV waves.
- The modified Born inversion not only smooths oscillating lobes which depend on the high frequency data, but also eliminates the errors due to mode conversions in inplane motions.

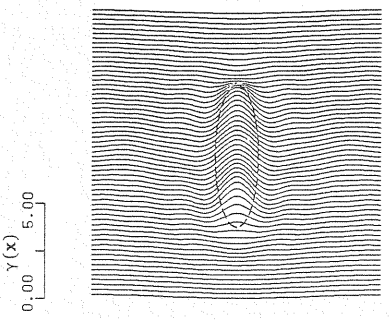

Fig. 9 Characteristic function of an elliptic cavity in a two dimensional space.

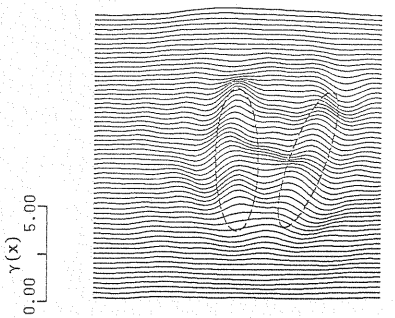

Fig. 10 Characteristic function of two adjacent elliptic cavities in a two dimensional space.

(2) Two dimensional problems

Firstly, we consider an elliptic cavity in a two dimensional space. The Born inversion method is applied to the following numerical data.

- The frequency up to $ak_T=10$ is taken into account (a : the half of the major axis of an ellipes).
- The distances from source and observation points to a center of a cavity are 5a.
- The pulse-echo scattering of P to P wave is generated at 60 points located equi-angularly around a cavity.

Fig. 9 shows the synthesized characteristic function $\gamma(\boldsymbol{x})$ of an elliptic cavity. Instead of a three dimensional plot of $\gamma(\boldsymbol{x})$, the height $\gamma(\boldsymbol{x})$ is laid vertically in a two dimensional plane. In this figure, the dashed curve indicates the original boundary to be determined. The shape of a cavity is well reproduced.

The second example is the case of adjacent elliptic cavities. Other numerical conditions are the same as in the last example. The result is depicted in Fig. 10. Although the boundaries located in the shadow zone of an incident wave are a little ambiguous, the shapes of cavities are also reproduced.

6. CONCLUDING REMARKS

In this paper, we formulated the Born inversion procedure for elastic waves scattered by a cavity and proposed the modified Born inversion for high frequency data. In numerical examples, an extensive study on several parameters (band limiting, angle between source and observation, mode conversion etc.) was made using the one dimensional inversion algorithm. Particularly, it was found that the modified Born inversion improves the results very much by eliminating the errors attributable to mode conversions as well as to high frequency data. In two dimensional examples, the shapes of elliptic cavities were well reproduced.

Although we demonstrated the inversion technique only for the scattered waves by cavities, the method proposed in the present paper is also available for elastic waves scattered by inclusions. In fact, the scattered wave due to an inclusion V is precisely expressed as follows[14],

$$u_i^{sc}(\boldsymbol{x}_B)=\int_V \{\Delta\rho\omega^2 U_i^k(\boldsymbol{x}_B,\boldsymbol{y})\,u_k(\boldsymbol{y})-\Delta C_{kjmn}U_i^{m,n}(\boldsymbol{x}_B,\boldsymbol{y})\,u_{k,j}(\boldsymbol{y})\}\,dS_y \quad \cdots\cdots (19)$$

where $\Delta\rho$ and ΔC_{kjmn} are the perturbations of mass density and elastic moduli in an inclusion from those in a surrounding medium. Eq. (19) has the similar form to eq. (13) derived for a cavity. Therefore, we can solve the inverse problems for inclusions, using the same procedure as in the case of a cavity. Currently we are testing the inversion method with experimental data both for cavities and inclusions on the basis of numerical results in this work.

REFERENCES

1) Pao, Y.-H. : Elastic waves in solids, J. Appl. Mech., 50 th Anniversary Issue, Vol. 50, pp. 1152~1164, 1983.
2) Kobayashi, S. and Nishimura, N. : Transient stress analysis of tunnels and caverns of arbitrary shape due to travelling waves, In

: Developments in Boundary Element Methods 2, Applied Science, Barking, pp. 177～210, 1982.

3) Kobayashi, S. : Some problems of the boundary integral equation method in elastodynamics, In : Boundary Elements, Springer, pp. 775～784, 1983.
4) Niwa, Y., Hirose S. and Kitahara, M. : Application of the boundary integral equation (BIE) method to transient response analysis of inclusions in a half space, Wave Motion, Vol. 8, pp. 77～91, 1986.
5) Langenberg, K. J., Brück, D. and Fischer, M. : Inverse scattering algorithms, In : New Procedures in Nondestructive Testing, Springer, Berlin, pp. 381～391, 1983.
6) Lewis, R. M. : Physical optics inverse diffraction, IEEE Trans. Antennas and Propagation, AP-17, pp. 308～314, 1969.
7) Bojarski, N. N. : A survey of the physical optics inverse scattering identity, IEEE Trans. Antennas and Propagation, AP-30, pp. 980～989, 1982.
8) Bleistein, N : Direct image reconstruction of anomalies in a plane via physical optics farfield inverse scattering, J. Acoust. Soc. Am., Vol. 59, pp. 1259～1264, 1976.
9) Bleistein, N. : Mathematical Methods for Wave Phenomena, Chap. 9, Academic Press, Orlando, 1984.
10) Achenbach, J. D., Viswarathan, K. and Norris, A. : An inversion integral for crack-scattering data, Wave Motion, Vol. 1, pp. 299～316, 1979.
11) Rose, J. H. and Krumhansl, J. A. : Determination of flaw characteristics from ultrasonic scattering data, J. Appl. Phys., Vol. 50, pp. 2951～2952, 1979.
12) Hsu, D. K., Rose, J. H. and Thompson, D. O. : Reconstruction of inclusions in solids using ultrasonic Born inversion, J. Appl. Phys., Vol. 55, pp. 162～168, 1984.
13) Gubernatis, J. E., Domany, E., Krumhansl, J. A. and Huberman, M. : The Born approximation in the theory of the scattering of elastic waves by flaws, J. Appl. Phys., Vol. 48, pp. 2812～2819, 1977.
14) Gubernatis, J. E., Domany, E. and Krumhansl, J. A. : Formal aspects of the theory of the scattering of ultrasound by flaws in elastic materials, J. Appl. Phys., Vol. 48, pp. 2804～2811, 1977.

(Received November 7 1985)